V International Scientific and Technical Conference Actual Issues of Power Supply Systems

# Dynamic Analysis of Capacitive Sensors for Water Flow Measurement in Large-Diameter Pipes

AIPCP25-CF-ICAIPSS2025-00257 | Article

# Dynamic Analysis of Capacitive Sensors for Water Flow Measurement in Large-Diameter Pipes

Farrux Kucharov [a)], Rustam Baratov, Bakhitbek Usnatdinov, Jahongir Jumaniyozov

*"Tashkent institute of irrigation and agricultural mechanization engineers" National Research University, Tashkent, Uzbekistan*

[a)] *Corresponding author: farrux.kocharov@mail.ru*

**Abstract.** Accurate water flow measurement in large-diameter pipes remains challenging due to turbulent and unsteady flow, non-uniform velocity profiles, air bubbles, and pressure fluctuations. Capacitive sensors are a promising solution for such conditions because of their simplicity, low power consumption, and high sensitivity potential. This study presents a theoretical and experimental investigation of the dynamic behavior of a capacitive water flow measurement sensor. The sensor response to rapid input signal variations was analyzed by modeling dynamic flow effects with a unit pulse. Transient processes were studied using the Laplace transform method, and the amplitude - frequency and phase - frequency responses of the sensor were derived. Numerical simulations were conducted in MATLAB and ISIS Proteus, and the results were validated through laboratory experiments on a prototype measurement circuit.

## INTRODUCTION

Despite the development of numerous high-accuracy methods and instruments for water flow measurement in irrigation systems, accurate flow measurement in large-diameter pipes (1– 4 meter) at major pumping stations remains a significant scientific challenge. Numerous studies indicate that conventional flow measurement methods, including ultrasonic, optical, acoustic, electromagnetic, and pressure-based flow meters, exhibit significant limitations when applied to large-diameter pipes [1].

Water flow measurement in large-diameter pipes is associated with several fundamental challenges, including non-uniform velocity distributions, complex asymmetric or vortex-type turbulent flow profiles, extremely high Reynolds numbers, the presence of air bubbles, sharp pressure and flow-rate fluctuations, and reverse flow. These factors result in a significant reduction in measurement accuracy. Furthermore, the design of calibration test facilities for such large-diameter pipes is highly complex, and no self-calibration methods currently exist for systems of this scale.

## RELATED RESEARCH WORKS

In practice, however, water flow measurements in large pumps and pumping stations remain largely based on nomograms, which leads to considerable measurement uncertainty.

Accurate water flow measurement in large-diameter pipes is essential for reliable determination of electrical energy consumption and overall efficiency at large pumping stations. Accurate water flow measurement is also required for reliable electronic monitoring of specific electrical energy consumption per unit volume of water, which directly influences the production cost of agricultural products.

According to statistical data, 74% of the total expenses required to supply consumers with each cubic meter of irrigation water is accounted for by electrical energy [2].

Therefore, in order to determine the actual value of electrical energy consumption at large pumping stations, it is necessary to optimize the operating modes of the pumps based on the irrigation norms of the agricultural crops being irrigated.

Accordingly, an urgent research task is the development of technically simple, high-accuracy water flow sensors with self-calibration, high sensitivity, low power consumption, and adaptive capability for operation in large-diameter pipes characterized by complex velocity profiles, turbulence, and unsteady flow conditions. This development should be based on the integration of digital technologies, artificial intelligence capabilities, and advanced sensor systems.

During the research, water-flow sensors operating on various principles were analyzed, including the following:

"**Ultrasonic water-flow sensors** - although they offer non-contact measurement, do not create additional hydraulic resistance in the pipe, have negligible pressure loss, are easy to install, and possess a wide measurement range along with other favorable technical characteristics, they also have certain limitations. For example, they are highly sensitive to air bubbles and various mixtures in the water; during turbulent flow, it is very difficult to estimate the average flow rate; and measurements are significantly inaccurate when the pipe is not completely filled [3, 4, 5, 6, 7]. **Electromagnetic (magneto-inductive)** flow sensors are highly reliable, have no moving parts, and their readings are independent of water's viscosity, temperature, density, and pressure. However, these systems are characterized by large physical dimensions, high sensitivity to external electromagnetic interference, the need for specialized noise-suppression circuitry, and frequent calibration requirements [1,8]. **Differential pressure (head-loss) flow meters**, one of the classical measurement methods, are simple in principle and widely used. Nevertheless, this method exhibits significant measurement errors under turbulent flow conditions, in the presence of vortices, or when the pipe is not fully filled. Due to these limitations, their use is often restricted [4, 7].

Recent studies suggest that capacitive sensors are a promising solution for water flow measurement in large-diameter pipes, largely satisfying the established technical requirements. They exhibit high sensitivity and possess a linear static characteristic.

However, capacitive sensors generate very weak electrical signals corresponding to water flow, which necessitates the design of measurement circuits capable of precise detection of extremely small capacitances. Currently, various methods exist for the measurement of extremely small capacitances (picofarad or nanofarad range), and the resulting signals are processed by microcontrollers or computers. However, ensuring high accuracy, minimizing external interferences, and reducing measurement errors remain critical challenges in the measurement of extremely small capacitances [2].

In real-time measurement and monitoring, it is essential to account for even very small capacitance variations. In such cases, it is crucial that the sensing element exhibits a linear static characteristic or that its associated accuracy is ensured. Furthermore, the design of an electrical measurement circuit with high resolution, as well as the careful selection of each of its components, is subject to strict requirements. To meet these requirements, several high-resolution methods for small capacitances measurement have been developed to date. In the following, we analyze some of the most commonly used techniques.

The method based on the principle of double differentiation is widely used as an effective approach for very low capacitances measurement, offering high accuracy [9,10]. Figure 1 below presents the block diagram of this measurement method.

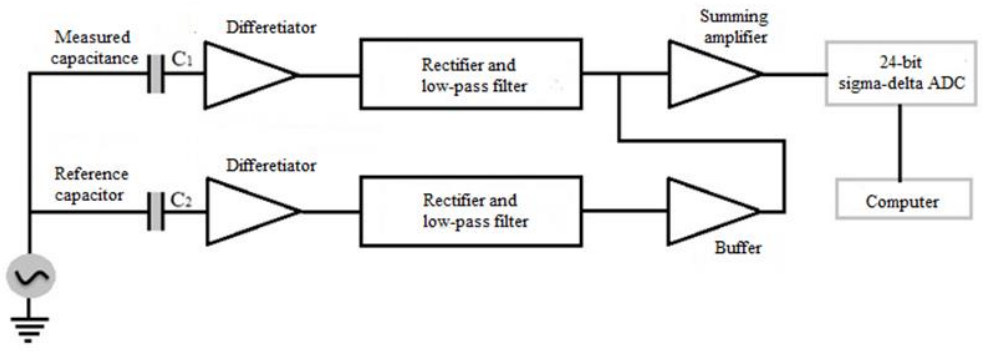


**FIGURE 1.** Block diagram of a low capacitance measurements system based on a double-differentiation method

This circuit can operate effectively over a capacitance variation range of up to $\Delta C = 10^{-18}$ F. It is particularly convenient for measurement and monitoring objects with unknown initial capacitance, and its design is relatively simple. However, due to the use of a 24-bit ADC and a reference capacitor, the cost of the system is high.

Furthermore, the use of a reference capacitor requires compliance with specific environmental conditions, which limits the application scope of this circuit.

Another method for low capacitances measurement, which offers high resolution and a high degree of linearity, is also available [11]. This capacitance measurement method can be widely applied in the field of biomedical engineering.

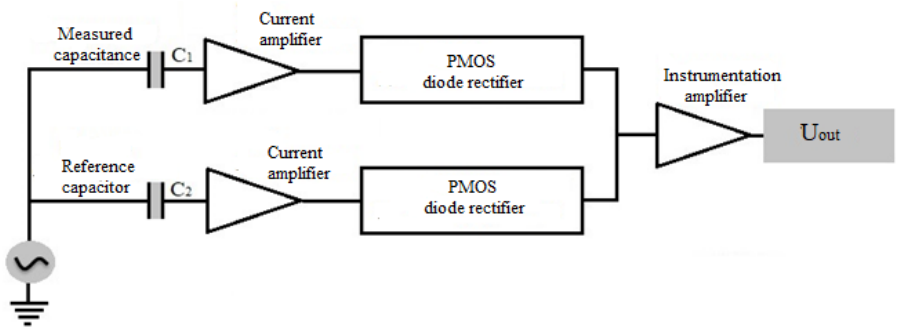


**FIGURE 2**. Block diagram of a ultra-low capacitance measurement method with high resolution and linear characteristics

Figure 2 shows the block diagram of a capacitance measurement method with high resolution and a linear characteristic [11,12]. This circuit is highly effective for extremely low capacitances measurement, specifically in the femtofarad range (1 fF = $10^{-15}$ F). Consequently, it is widely applied in medical diagnostic equipment. However, this method also relies on a reference capacitor and the use of alternating current, making it susceptible to external electromagnetic field interference.

Another recent method for measuring extremely low capacitances involves using a novel signal generator equipped with a third-order high-frequency filter that exhibits very low sensitivity to low or high-frequency components of the signal [10,13,14,15,16].

In this method, a CMOS circuit, developed using integrated circuit technology with a feature size of 0.7 μm, is employed. The reference capacitance is 2 pF, and over a temperature range from −30 °C to +70 °C, the measurement error is as low as 100 aF (1 aF = $10^{-18}$ F). Figure 3 presents the block diagram of this measurement method.

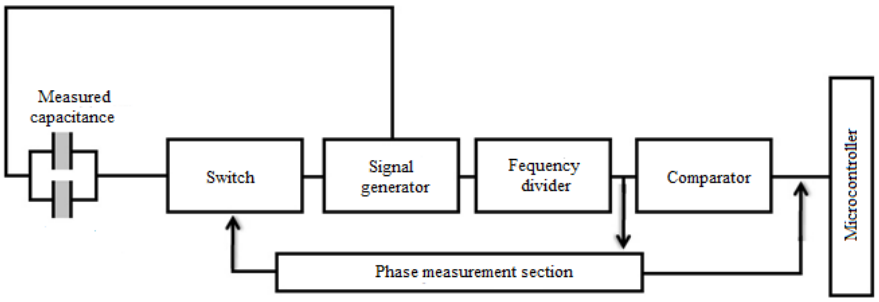


**FIGURE 3.** Block diagram of a ultra-low capacitance measurement system using a signal generator

This circuit, utilizing a reference capacitor, features automatic calibration to minimize both multiplicative and additive errors. The output of the measurement circuit is independent of the signal amplification factor, and temporal fluctuations of the signal do not affect the output. The measurement range is 0÷2 pF, with a sampling time of 330ns.

Another method for measuring extremely small capacitances is based on a linear relationship between the phase shift of the output signal and changes in the phase angle [16,17,18,19,20]. One of the main features of this circuit is its high immunity to parasitic signals, along with very high resolution. Figure 4 shows the block diagram of this method for extremely low capacitances measurement.

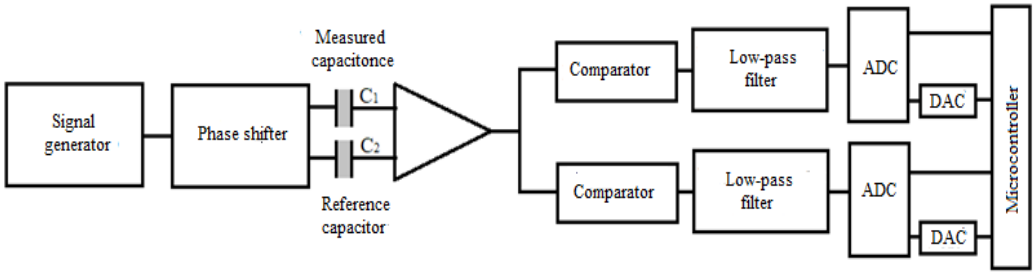


**FIGURE 4.** Block diagram of a ultra-low measurement system based on phase angle

The static characteristic of this circuit exhibits a nonlinearity of 0.5%. Compared to other measurement circuits, its main advantages are the linearity of its static characteristic and its high resolution. This circuit is primarily used for extremely low displacements measurement of various objects, down to $7.7 \times 10^{-12}$ m.

Another method for measuring low capacitances is based on phase delay in an RC network [21,22,23]. Figure 5 shows the block diagram of this measurement method.

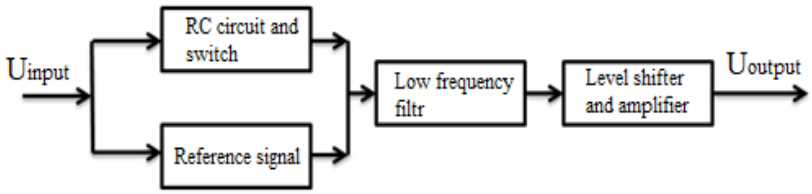


**FIGURE 5.** Block diagram of a capacitance measurement method based on RC phase delay

The output of this RC network serves as a pulse-width modulation (PWM) signal, with each measurement cycle being proportional to the capacitance variation. The sensitivity of this measurement circuit is approximately 246 mV/pF. The output signal is filtered through a low-pass filter, level-adjusted, and amplified. Therefore, this method is suitable for capacitances measurement of several tens of pF or smaller. Moreover, this measurement approach requires few components and has a simple circuit design.

When using capacitive sensors, their main characteristics are the amplitude-frequency response (AFR) and phase-frequency response (PFR). These characteristics are used, in particular, to evaluate the following properties of capacitive sensors:

- frequency characteristic: capacitive sensors are used across various frequency ranges, and their amplitude-frequency response (AFR) is employed to assess the frequency range in which the sensor operates stably or with minimal deviation;

-evaluation of resonance effects: in some cases, a capacitive sensor may operate in a resonant state, which can affect measurement accuracy. Therefore, the amplitude-frequency response (AFR) is also important for detecting the occurrence of unwanted vibrations;

-evaluation of phase shift: in capacitive sensors, the phase shift or time delay of the signal is assessed using the phase-frequency response (PFR). This is particularly important for ensuring high measurement accuracy and in systems with feedback loops.

-signal processing optimization: when electronic components such as filters and amplifiers are present in the measurement circuit, the amplitude-frequency response (AFR) and phase-frequency response (PFR) are used to tune the system characteristics to an optimal operating mode;

-error correction and calibration: if the static characteristic of a capacitive sensor exhibits nonlinearity or frequency-dependent deviations, corrections can be applied using the amplitude-frequency response (AFR) or phase-frequency response (PFR), or through software-based methods;

- proper circuit selection: some capacitive sensors perform optimally only within a specific frequency range. This frequency range can be determined using the amplitude-frequency response (AFR) or phase-frequency response (PFR).

Therefore, we analyze the amplitude-frequency response (AFR) and phase-frequency response (PFR) of the capacitive sensor used for water flow measurement.

## MATERIALS AND METHODS

Next, the measurement circuit diagram of the capacitive sensor shown in Figure 6 is analyzed. For this circuit, the following expression can be written:

$$U_{input}(t) = U_R(t) + U_c(t) = i(t) \cdot R + \frac{1}{C}\int i(t)dt \quad (1)$$

The effect of the input signal on the measurement circuit of any measurement and control sensor depends directly on the frequency of the input signal [24, 25, 26]. In investigating such a process, a unit pulse or Dirac function (see fig.6 a) is applied to the input of the measurement chain, and the chain's response is observed.

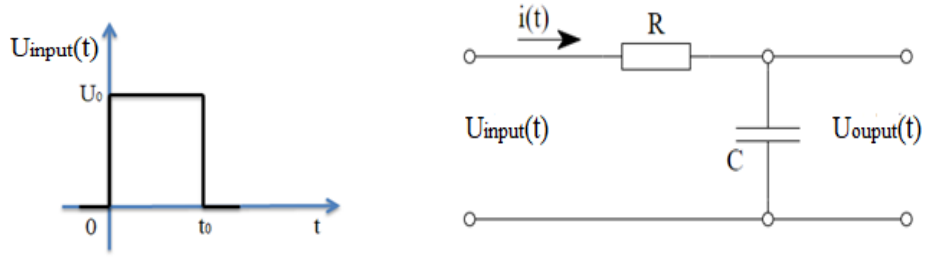


**FIGURE 6**. Unit pulse or Dirac function (a) and integrating circuit (b)

The nature of the circuit's response depends on several parameters, such as the amplitude and duration of the unit pulse [27, 28, 29]. Therefore, to the input of the measurement circuit shown in Figure 6 (b) above, we apply a unit pulse voltage (signal) as illustrated in Figure 6 (a).

For the analysis of transient processes, the Laplace transform method is used. Therefore, we depict the measurement circuit in operator form, as shown in Figure 7, (a). In this diagram, $U_{input}(t)$ is considered the input voltage, while $U_{output}(t)$ is regarded as the response voltage. We then write the operator form of the transfer coefficient in terms of voltage:

$$K_U(p) = \frac{U_{output}(p)}{U_{input}(p)} \quad (2)$$

According to Ohm's law, the current is expressed as follows:

$$I_1(p) = \frac{U_{input}(p)}{Z_R(p)+Z_C(p)}, \quad (3)$$

The output voltage of the measurement circuit can be written as follows:

$$U_{output}(p) = Z_C(p) \cdot I_1(p) = \frac{Z_C(p)\cdot U_{input}(p)}{Z_R(p)+Z_C(p)}, \quad (4)$$

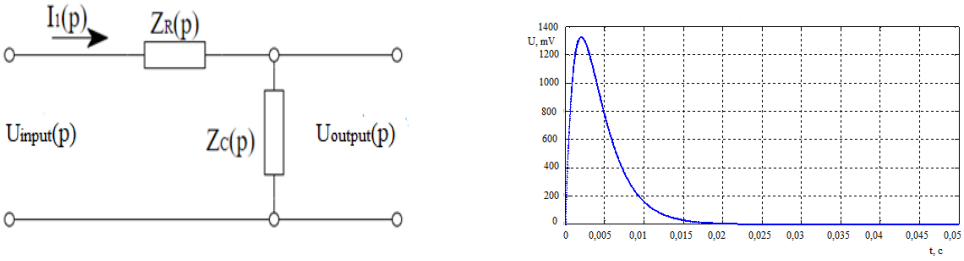


(a) (b)

**FIGURE 7**. Laplace transformed circuit (a), and response to a unit pulse (b)

Alternatively, the operator form of the transfer coefficient is equal to the following:

$$K_U(p) = \frac{U_{output}(p)}{U_{input}(p)} = \frac{I_1(p)\cdot Z_C(p)}{I_1(p)(Z_R(p)+Z_C(p))} = \frac{Z_C(p)}{(Z_R(p)+Z_C(p))}, \quad (5)$$

If we substitute the values of the operator resistances Z(p) into equation (5) and divide each term by RC, the following expression is obtained:

$$K_U(p) = \frac{\frac{1}{pC}}{R+\frac{1}{pC}} = \frac{1}{pRC+1} \quad (6)$$

Using the Laplace transform, we move from the operator description to the time-domain characteristic. Taking into account that $\frac{1}{p+\alpha} = e^{-\alpha t}$we can write the following pulse response:

$$h(t) = \frac{1}{RC}\cdot e^{-\frac{t}{\tau_3}}, \quad (7)$$

Here, $\tau_3 = RC$- the time constant of the measurement circuit.

To determine the transient response characteristic, we write the following expression:

$$F(t) = \int_0^{t_0} h(t)dt = \frac{1}{RC}\int_0^{t_0} e^{-\frac{t}{\tau_3}}dt = 1 - e^{-\frac{t}{\tau_3}}, \quad (8)$$

To determine the output voltage, we analyze the following two time intervals:

1) $0 \le t \le t_0$ in this case

$$U_{output}(t) = \int_0^t U_{input}(\tau)h(t-\tau)d\tau = \frac{U_0}{RC}\int_0^t e^{-\frac{(t-t_0)}{\tau_3}}d\tau \quad (9)$$

By substituting the variable, or $t-\tau = \varphi$ and $d\tau = -d\varphi$ taking into account the change of the integration limit, we write the following:

$$U_{output}(t) = -\frac{U_0}{RC}\int_0^t e^{-\frac{\varphi}{\tau_3}}d\varphi = \frac{U_0}{RC}\int_0^t e^{-\frac{\varphi}{\tau_3}}d\varphi = U_0\left(1 - e^{-\frac{t}{\tau_3}}\right). \quad (10)$$

In this case, at the end of the pulse, the output voltage of the measurement circuit is equal to the following value:

$$U_{output}(t_0) = U_0(1 - e^{-\frac{t}{\tau_3}}). \quad (11)$$

2) $t \ge t_0$ when or $t = t_0$ at $U_{input}(t)$ . The function has a discontinuity, so it is necessary to perform the integration over two intervals: from 0 to $t_0$ and from $t_0$ to the current $t$. Therefore, we write the following expression:

$$U_{output}(t) = \int_0^{t_0} U_{input}(\tau)h(t-\tau)d\tau + \int_{t_0}^t U_{input}(\tau)h(t-\tau)dt \quad (12)$$

Thus, by substituting the corresponding time interval values for $U_{input}(t)$, we obtain the following:

$$U_{output}(t) = \int_0^{t_0} U_0 h(t-\tau)\,d\tau + \int_{t_0}^t 0\cdot h(t-\tau)dt = \frac{U_0}{RC}\int_0^{t_0} e^{-\frac{t}{\tau_3}}d\tau = \frac{U_0}{RC}\cdot e^{-\frac{t}{\tau_3}}\int_0^{t_0} e^{\frac{t}{\tau_3}}d\tau = U_0\cdot e^{-\frac{t}{\tau_3}}\left(e^{\frac{t}{\tau_3}} - 1\right) \quad (13)$$

Using a step function and assuming the initial time state as $t = t_0$, we write the following:

$$U_{output}(t) = U_0\left(1 - e^{-\frac{t_0}{t_3}}\right)\cdot e^{-\frac{(t-t_0)}{t_3}} \quad (14)$$

Using formula (14), we plot the unit impulse response of the measuring circuit. The corresponding graph is shown in Figure 7, (b).

As noted above, in order to construct the amplitude-frequency and phase-frequency response of the integrating circuit, we express the complex form of its transfer coefficient:

$$K_{t.c.}(j\omega) = \frac{\underline{U}_{output}}{\underline{U}_{input}} = \frac{\frac{1}{j\omega C}\underline{I}}{(R+\frac{1}{j\omega C})\cdot\underline{I}} = \frac{\frac{1}{j\omega C}}{1+\frac{1}{j\omega C}}, \quad (15)$$

Here, the complex transfer coefficient of the $K_{t.c.}(j\omega)$-integrating circuit.
The magnitude of formula (15) is given by the following expression:

$$|K_i(f)| = \frac{1}{\sqrt{1+(\omega RC)^2}} = \frac{1}{\sqrt{1+(\omega\tau)^2}}, \quad (16)$$

Equation (16) represents the amplitude-frequency response (AFR) of the low-capacitance measurement sensor. To construct its phase-frequency response (PFR), we utilize the following expression:

$$\varphi_i(f) = -arctg(\omega RC) = -arctg(\omega\tau) \quad (17)$$

This expression represents the phase-frequency response (PFR) of the low-capacitance measurement sensor.

Taking into account $f_c$ in the resulting formulas (16) and (17), $K_{t.c.}(f)$ can be expressed as follows.:

$$|K_{t.c.}(f)| = \frac{1}{\sqrt{1+\left(\frac{f}{f_c}\right)^2}} \quad (18)$$

where $f_c$ – cutoff frequency, f – frequency of the input signal.

Based on equations (16) - (18), the magnitude and phase frequency responses of the low-capacitance measurement sensor are derived.These are shown in Figure 8, (a) and (b) below.

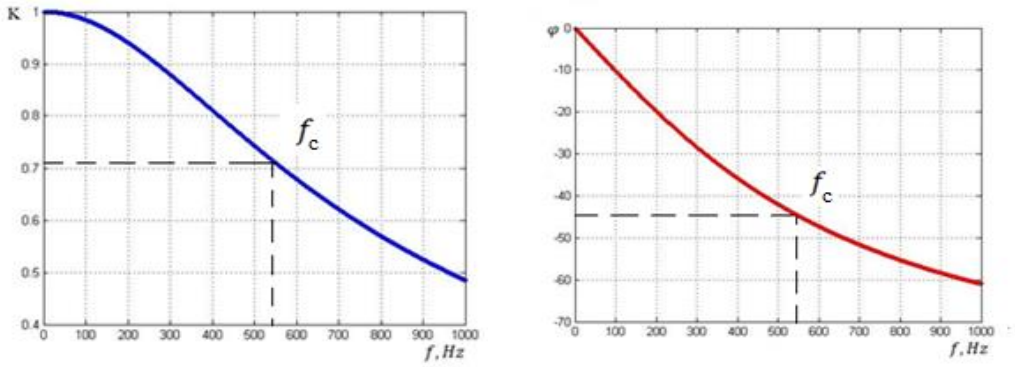


(a) (b)

**FIGURE 8**. Frequency response of the capacitive sensor: (a) amplitude-frequency response, b) phase-frequency response

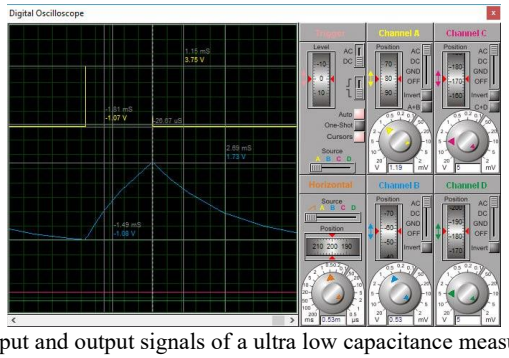


**FIGURE 9**. Input and output signals of a ultra low capacitance measurement circuit

As shown in Fig. 8, analysis of the AFR and PFR demonstrates that at frequencies above the cutoff frequency fc, the magnitude of the transfer function $|K_{t.c}(f)|$ tends to zero and the phase approaches 90°. Hence, the circuit can be

classified as a low-pass filter with a passband from 0 to fc, where fc corresponds to a −3 dB attenuation ($|K_{t.c}|$ = 0.707). Simulation results obtained in MATLAB for the proposed integrated circuit were compared with those obtained using ISIS Proteus, as shown in Fig. 9.

## EXPERIMENTAL RESEARCH

To verify the adequacy of the theoretical results, a laboratory prototype of the capacitive sensor measurement circuit was assembled and experimentally evaluated. A unit pulse was applied to the circuit input using an FY6900 signal generator, while the output signal waveforms and amplitudes were measured with a FLUKE 199 SCOPEMETER. The excitation frequency was varied in the range of 100 -1000 Hz.

The unit-impulse response of the measurement circuit was analyzed using MATLAB and ISIS Proteus. Experimental studies were then performed to validate the theoretical results, and the corresponding experimental setup and circuit schematics are presented in Fig. 10.

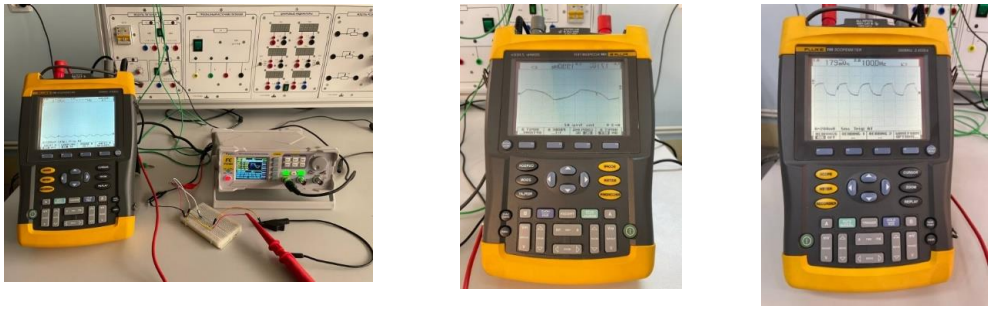

**FIGURE 10**. Experimental setup of the measurement circuit

Figure 11 below presents the amplitude - frequency and phase - frequency responses obtained experimentally.

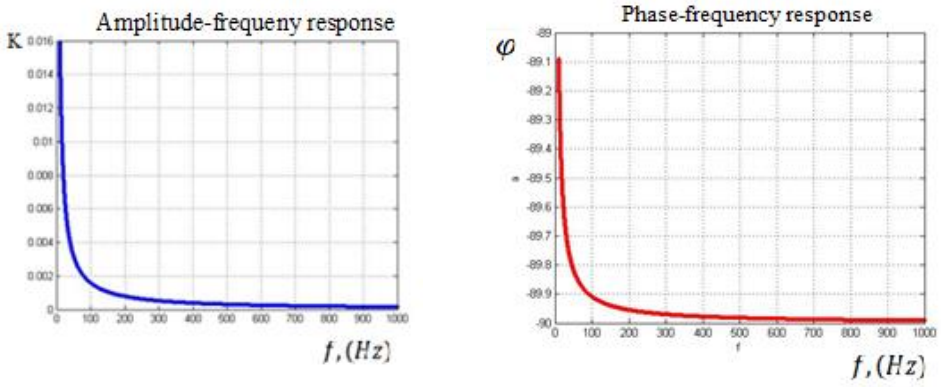


(a) (b)

**FIGURE 11**. Experimental results of the RC integrator circuit: (a) amplitude-frequency responce (b) phase-frequency responce

## CONCLUSIONS

This study investigated the feasibility of using capacitive sensors for water flow measurement and analyzed their dynamic characteristics. In particular, the sensor response was examined under conditions of rapid input signal variations caused by dynamic flow effects, including turbulence, frequent formation of asymmetric and swirling flow profiles, air bubble entrainment, and abrupt fluctuations in pressure and flow rate. These rapid input variations were modeled using a unit impulse, enabling analysis of the sensor's dynamic behavior and the transient response of

the measurement circuit. Furthermore, the amplitude - frequency and phase-frequency responses of the capacitive sensor under dynamic conditions were investigated both theoretically and experimentally. The obtained results can be used to determine the frequency range that ensures accurate measurements, evaluate deviations of the output signal from nominal values, and assess measurement stability under dynamic operating conditions. The findings are also valuable for the design of capacitive sensors, optimization of measurement circuit parameters in dynamic regimes, and the development of effective filtering techniques to mitigate noise induced by external environmental factors.

## REFERENCES

1. Iñigo Albaina, Iñigo Bidaguren, Urko Izquierdo, G.A.Esteban. Influence of Various Accessories Upstream Large Water Meters.// Water Resources Management, *(2023) 37:4693–4708* https://link.springer.com/article/10.1007/s11269-023-03573-2

2. Baratov, R., F Kucharov. Capacıtıve sensors wıth ultra-small capacıtance for smart measurement and control systems. // (2024). E-ISSN: 2181-1105, DOI: https://doi.org/10.59048/2181-1105.1603

3. Lin Li, Ye Zhou, Beibei Xu, Hongli Zhao and Yuntao Ye. Enhancing Accuracy of Ultrasonic Transit-Time Flow Measurement in Hydropower Systems Under Complex Operating Conditions: A Comprehensive Review.// Machines 2025, 13, 713. https://www.mdpi.com/2075-1702/13/8/713

4. Jiwei Li, Lingyun Qiu, Zhongjing Wang, Hui Yu. An Acoustic Inversion-Based Flow Measurement Model in 3D Hydrodynamic Systems.// Feasibility study of flow measurement method. March 18, 2025 https://arxiv.org/abs/2503.11986

5. Akhmad Afandi, Khasani, Deendarlianto, I.G.N.B. Catrawedarma, Setya Wijayanta. The development of the ultrasonic flowmeter sensors for mass flow rate measurement: A comprehensive review.// Flow Measurement and Instrumentation, Volume 97, July 2024, 102614 https://www.sciencedirect.com/science/article/abs/pii/S0955598624000943#:~:text=To%20address%20these%20gaps%2C%20this,cell%20systems%20in%20the%20future

6. R. Ren, Hongliang Wang, Xiaolei Sun and He Quan. Design and Implementation of an Ultrasonic Flowmeter Based on the Cross-Correlation Methods, Sensors 2022, 22, 7470. https://www.researchgate.net/publication/364296571_Design_and_Implementation_of_an_Ultrasonic_Flowmeter_Based_on_the_Cross-Correlation_Method/link/68070c31bd3f1930dd624457/download

7. Mohammadhadi Mesmarian, Mohammad Mahdi Kharidar, Hossein Nejat Pishkenari. Development of a Transit-Time Ultrasonic Flow Measurement System for Partially Filled Pipes: Incorporating Flow Profile Correction Factor and Real-Time Clogging Detection.// Preprint version – submitted to IEEE Sensors Journal, *2025)* https://arxiv.org/abs/2511.19310

8. Stefan Kaltenbacher, Martin Steinberger, Martin Horn. Pipe Roughness Identification of Water Distribution Networks: A Tensor Method.// Inffeldgasse 21b, 8010 Graz, November 13, 2019, Austria. https://export.arxiv.org/pdf/1908.07794v2

9. Preethichandra D.M.G., Katsunari Shida. A Simple Interface circuit to measure Very Small Capacitance Changes in Capacitive Sensors, IEEE, Trans. Instrum. Meas., Vol.50, Dec. 2001, pp.1583-1586.

10. M.R.Haider, M.R.Mahfouz, S.K.Islam, S.A.Eliza, W.Qu, E.Pritchard. A low-power Capacitance measurement Circuit with High Resolution and High Degree of Linearity, IEEE, Circuits and Systems, Sep. 2008, pp.261-264.

11. Junjie Y., Shuai L., Li L., Ruiqi B., Shuo Ch., Hanyang G. Wire-mesh sensor technique for void fraction measurement in gas–liquid two-phase flow under varying conductivity conditions// Measurement – journal. Ташкент - 2025, 256 (2025) 118281.

12. R. Dai, N. Jin, Q. Hao, W. Ren and L. Zhai. Measurement of Water Holdup in Vertical Upward Oil–Water Two-Phase Flow Pipes Using a Helical Capacitance Sensor// Sensors. 2022, 22, 690

13. Dhiraj Kumar, Aakash Dewangan, Rajiv Tiwari, D.J.Bordoloi. Identification of inlet pipe blockage level in centrifugal pump over a range of speeds by deep learning algorithm using multi-source data// www.elsevier.com/locate/measurement 186(2021) 110146 pp 5-8.

14. L. Han, M. Chen, X. Liu, Ch. Fu. New Measurement Method of Oil-Water Two-Phase Flow with High Water Holdup and Low Rate by Phase State Regulation.// MEASUREMENT SCIENCE REVIEW, 23, (2023), No. 6, 268-274. ISSN 1335-8871. DOI: 10.2478/msr-2023-0034

15. Suman Lata, H.K. Verma. Virtual capacitance meter based on ratio-metric voltage measurement for sensor testing.// Materials Today: Proceedings, 34 (2021) 575–581. ISSN 1335-8871. https://doi.org/10.1016/j.matpr.2020.01.200
16. Czaja Z., A New Approach to Capacitive Sensor Measurements Based on a Microcontroller and a Three-Gate Stable RC Oscillator, IEEE Transactions on Instrumentation and Measurement, Vol. 72 (2023), 2002009, DOI: 10.1109/TIM.2023.3244851
17. Van Kann F. J., Veryaskin A. V.A Novel Capacitance-to-Phase Transducer Based on a Simple Resonant Circuit.// Instrumentation and Detectors. *arXiv preprint*, 2023. URL: https://arxiv.org/abs/2310.04075
18. E. Ranjbar, M. B. Menhaj, A. A. Suratgar, J. A. Perez, M. Prasad. Design of a fuzzy PID controller for a MEMS tunable capacitor for noise reduction in a voltage reference source. SN Applied Sciences (2021) 3:609. https://doi.org/10.1007/s42452-021-04585-6.
19. I. Saied and M. Meribout. Electronic hardware design of electrical capacitance tomography systems. Phil. Trans. R. Soc. A 374: 20150331. http://dx.doi.org/10.1098/rsta.2015.0331
20. Jenn-Yih CHEN, Yi-Ling LIN, Bean-Yin LEE. Development of the Adaptive System for Tool Management. Technical Gazette 30, 2(2023), 648-654. ISSN 1330-3651 (Print), ISSN 1848-6339 . https://doi.org/10.17559/TV-20220702054333
21. Robert N.Dean and Aditi Rane. Improved Capacitence measurement Technique Based of RC phase delay. In Proceedings of the IEEE Instrum. Meas. Tech. Conf., 2010, pp. 367-370.
22. Rus T., Dular M., B.˘ Sirok, M. Ho˘ cevar, and I. Kern, "An investigation of the relationship between acoustic emission, vibration, noise, and cavitation structures on a Kaplan turbine," Journal of Fluids Engineering, vol.129, no. 9, 2007 pp. 1112–1122.
23. W. Ahmed, A. Fatayerji, A. Elsaftawy, M. Hassan, D. Weaver and J. Riznic . A New Capacitance Sensor for Measuring the Void Fraction of Two-Phase Flow Through Tube Bundles// Sensors. 2020, doi:10.3390/s20072088
24. Baratov R.Zh., Chulliev Ya.E., Pardaev A.I., Abdullaev M.H. Software for an intelligent sensor for monitoring and measuring liquid and gas pressure in pipelines // Registered with the Intellectual Property Agency under the Ministry of Justice of the Republic of Uzbekistan, No. DGU 11167, dated 15 April 2021.
25. Q. Su, J. Li 1 and Z. Liu. Flow Pattern Identification of Oil–Water Two-Phase Flow Based on SVM Using Ultrasonic Testing Method// Sensors. 2022, 22, 6128. https:// doi.org/10.3390/s2216612
26. Y. Zhao, S. Yue, Y. Zhang, and H. Wang, "Flow velocity computation using a single ERT sensor," *Flow Meas. Instrum.*, vol. 93, no. July, p. 102433, 2023, doi: 10.1016/j.flowmeasinst.2023.102433.
27. W. Guo, C. Liu, and L. Wang, "Temperature fluctuation on pipe wall induced by gas–liquid flow and its application in flow pattern identification," *Chem. Eng. Sci.*, vol. 237, p. 116568, 2021, doi: 10.1016/j.ces.2021.116568.
28. J. Lu, 4, L. Liu, G. Chen, J. Li, Ch. Li and Y. Liu. Flow calibration method for gas-liquid two-phase flow of Coriolis flowmeter based on LSTM. // Journal of Physics: Conference Series. 2369 (2022) 012031. DOI 10.1088/1742-6596/2369/1/012031
29. Baratov, R., Begmatov, M., Mustafoqulov, A., Kucharov, F., Sabirov, E. Study on the methods of measuring power of the rotating mechanisms.// (2023). ISSN 25550403. DOI 10.1051/e3sconf/202343401014